SYSTEM IDENTIFICATION AND SLIDING MODE TRACKING CONTROL FOR ELECTRO-HYDRAULIC STEER-BY-WIRE SYSTEM

Magdy R. Roman [a,*], Sayed M. Shaaban [b], Mohamed G. Rabie [c], Mohamed H. Aly [a]

[a] Mechanical Power Engineering Department, Faculty of Engineering at Mataria, Helwan University, Cairo, Egypt
[b] Automotive and Tractors Engineering Department, Faculty of Engineering at Mataria, Helwan University, Cairo, Egypt
[c] Manufacturing and Production Technology Department, Modern Academy, Cairo, Egypt
[*]Corresponding author: magdy_roman@m-eng.helwan.edu.eg

ABSTRACT:

In passenger cars Steer-by-wire (SBW) system is a promising technology in which a control circuit replaces the mechanical link between the driving wheel and the vehicle's front wheels. This could improve the design flexibility and steering capability providing that the steering controller has a good tracking response to the driver's demand. In this research, a robust sliding mode control is designed and implemented to an electro-hydraulic SBW system. Grey-box system identification approach is used to identify the parameters of the driven mathematical model. The system is given a standard input signal, Pseudo Random Multi-level Sequence (PRMS), to be stimulated in the relevant bandwidth. Then, a robust sliding mode controller is designed, based on a fixed boundary layer, to provide system stability over a wide range of operating conditions and system disturbances. Finally, the algorithm is implemented experimentally in a real-time platform in order to evaluate the tracking performance. The test signals are designed based on the highest rate of steering provided by a human driver. The results proved the capability of the steering system to track the driver's demand accurately. At high steering rate conditions (720 degree/s) the maximum overshoot is found to be 3% with a setling time of 0.1 s.

Keywords: Electro-hydraulic position tracking, Sliding mode control, Gray-box system identification, Pseudo random multi-level sequence.

1. Introduction

Steer-by-wire (SBW) techniques, generally drive-by-wire (DBW), have been extensively considered both by academia and automotive industry over the last decade. In SBW system the traditional mechanical link connecting the driving wheel with the steering mechanism is removed and a control circuit with sensors and actuators is used instead. This provides several advantages over the traditional way such as more freedom in the cabin design, more safety [1], better vehicle dynamics, motility and stability [2]. Moreover, SBW system is crucial issue in the research and production of the autonomous car [3]. With no direct contact between the steering wheel and the car front wheels, it is necessary that the steering controller provides robustness and good tracking behavior to the steering commands.

Electro-hydraulic actuator (EHA) system has greatly expanded the range of applications for hydraulics in a variety of domains. This includes air vehicles [4], automobiles [5, 6], excavators [7], manufacturing processes [8–10] and many others. EHA is applied in SBW systems as well, especially because EHA systems possess a high power-to-weight ratio [11]. They also have the capacity to produce various speeds, step-less motion, capability to produce high force levels and precisely implementation. On the other side, due to oil leakages and compressibility in the proportional and servo valves, significant nonlinearities exist in the EHA systems dynamics. When applied in steer-by-wire systems the EHA experiences nonlinear disturbances produced by the tire-road interaction.

Achieving a good tracking behavior for the steer-by-wire system necessitates the existence of a good quality model that can present system dynamics. Modeling is a vital issue in scientific research. In most circumstances, the mathematical model can be derived straightforward from physical principles. This model, however, contains many parameters that need to be approximated. Some of the parameters may be found in electro-hydraulic steering system involve mass and moment of inertia, spool dimension, oil properties, coefficients of friction, flow, and leakage, etc. Such parameters are generally measured in labs using a variety of costly instruments and measurements.

System mathematical model can be achieved alternatively using system identification approaches. This necessitates the acquisition of a set of well-prepared input-output data that describe all the dynamic behavior of the system. In black-box system identification a previous understanding about the system model is not required. Yet, candidates of model structures are tested and the best performer is picked up. On the other side, grey-box system identification uses physically derived model structures and only identifies the model parameters. It usually leads to models which are easier to physically understand and have greater generalization characteristics than the models obtained by black-box identification [12].

Different control strategies for EHA position tracking system are widely investigated in literature. Based on local linearization of nonlinearities, methods such as pole placement [13, 14], traditional PID [15], and adaptive control [16], have already been implemented. Ghazali proposed a linear-quadratic regulator (LQR) and zero-phase-error tracking control (ZPETC) [17]. The algorithm was simple and effective in handling non-minimum zero-phase linear systems. Local linearization-based controllers work well providing that the system operation is within a small range of a nominal operating state.

Other approaches were adopted in literature to deal with nonlinearities found in EHA systems. Seo, Mintsa, and Vossoughi proposed a feedback linearization to cancel the system nonlinearities [18-20]. Whereas feedback linearization is a very straightforward nonlinear technique, it does need the use of a well-known system model to assure that the tracking error is exponentially converged. Liccardo and Çimen used State-Dependent Riccati Equation (SDRE) to provide an optimal control approach [21, 22]. The SDRE approach captures nonlinearities by transforming the nonlinear system into a linear structure with state-dependent coefficient (SDC) matrices while minimizing a nonlinear performance index with a quadratic-like structure. When applied to an EHA system, SDRE demonstrated good tracking control performance, with the highest amplitude error being 3e-5 m and the actuator phase lag being 0.035 s. Kim and Ahn utilized position tracking controllers based on backstepping algorithm and implemented [23, 24]. Tri suggested a hybrid of modified backstepping algorithm supported by an iterative learning method to adaptively accomplish tracking [25].

Position tracking behavior would considerably be degraded by system uncertainties and external disturbances [26]. This motivated several researchers to develop compensating approaches. Wonhee and Guo used disturbance observer-based controllers for position tracking of EHA, since it is not always feasible to measure disturbances directly in practice [27, 28]. Other researchers proposed sliding mode control (SMC) to account for system disturbances and uncertainties [29-33]. Due to its robustness against uncertainties and external disturbances, SMC has effective and simple approach for controlling nonlinear systems with uncertainties. SMC is a kind of Variable Structure Control in which the state of the system is manipulated to get to a sliding surface and then confined to it by a certain control law that changes value according to a predefined switching rule. When the system is constrained in this surface, its dynamic behavior is described as the ideal sliding mode which can be tailored, from the design point of view, by suitably choosing the sliding surface. However, in classic sliding mode control, the discontinuous term generates chattering, which is extremely undesired [34]. A well-known and simple solution for chattering reduction is using the boundary layer approach [35].

Electro-hydraulic steer-by-wire system is such a complex electro-hydro-mechanical system with inherent nonlinearities and nonlinear external disturbances (caused by the tire-road interaction). The main contribution of the current research is to provide a simple, yet effective and robust, modeling and control of the electro-hydraulic steer-by-wire system. The system modeling is based on grey-box system identification techniques. The identified model is then used to design a sliding-mode controller based on a fixed boundary layer and taking into account the maximum system disturbances. Finally, an experimental verification is done to verify the proposed controller performance at different operating conditions.

This paper is structured as follows. Section 2 describes the system description and modeling. System identification based on gray box approach is presented in Section 3. In Section 4, sliding mode controller is designed. Section 5 discusses the results and experimental verification. Finally, research conclusion is presented in Section 6.

2. System Description and Modeling

A schematic representation of the steering control system is depicted in Fig. 1. The steering wheel angle sensor sends steering signals to the controller. The later in turn generates the required control signal which controls the servo-solenoid valve so that the front wheel follow the driver's steering demands. LVDT sensor is used to measure the front wheel angle indirectly by measuring the displacement of the hydraulic actuator.

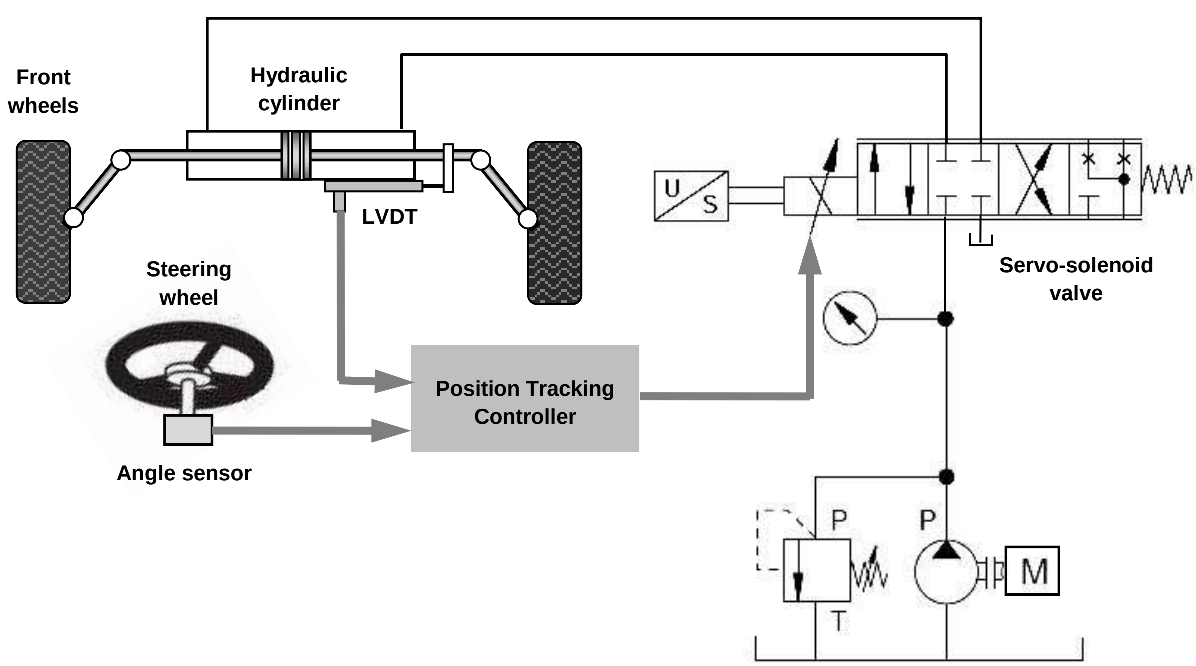

Fig. 1. Front-wheel angle control system using EHA

Starting from the physical laws can give us a particular insight into the system dynamics and properties. Fig. 2 shows a schematic diagram of the electro-hydraulic actuator system used for actuating the steering mechanism. By regulating the discharges Q_1 and Q_2, the actuator can be controlled precisely. However, the direct relation between the actuator displacement (piston displacement, x_p) and these discharges depends on the dynamic properties of the load acting on the piston. This is due to the internal leakages and the effect of the oil compressibility. According to the Newton's 2nd law, the force balance of the actuator is given as,

$$m\ddot{x}_p = A_p P_L - b\dot{x}_p - F_d, \tag{1}$$

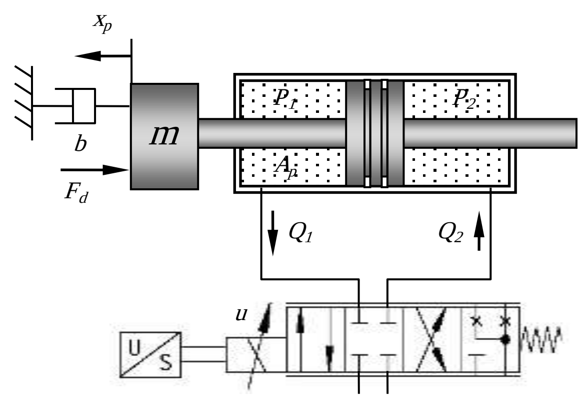

Fig. 2. Electro-hydraulic actuator system used for actuating the steering mechanism

where $P_L = P_1 - P_2$, is the load pressure [N/m^2], x_p is the displacement of the piston [m], m is the mechanism mass [kg], b is coefficient of viscous damping [N/(m/s)], A_P is the piston area [m^2], and F_d is the steering mechanism external forces caused by tire-road interaction [N]. By assuming symmetricity of the valve orifices and the orifice area varies linearly with the valve stroke [11], the load flow rate as a function of the displacement of the spool is given as,

$$Q_L = C_d w x_v \sqrt{\frac{1}{\rho}(P_s - \mathrm{sgn}(x_v) P_L)}\ , \tag{2}$$

where Q_L is the load-flow rate [m^3/s], x_v is the spool displacement [m], w is the spool area gradient [m], C_d is the coefficient of discharge, ρ is the density of the oil [kg/m^3], P_s is the supply pump pressure [N/m^2] and $\mathrm{sgn}(x_v)$ is the sign function of x_v.

Applying mass conservation to the cylinder, considering oil compressibility and leakage, the flow rate Q_L can be given as [11],

$$Q_L = A_P \dot{x}_p + C_t P_L + \frac{V_t}{4\beta_e}\dot{P}_L \tag{3}$$

where, A_P is the piston area, C_t is the coefficient of the total leakage [m^5/Ns], β_e is the oil bulk modulus [N/m^2] and V_t is the total actuator volume [m^3].
The relationship between the spool displacement x_v and the input voltage u is considered as,

$$x_v = u * k_v \tag{4}$$

where, k_v is the servo amplifier gain. This simplified relationship has good accuracy since the electro-mechanical solenoid dynamics is fast enough and, thus, can be neglected compared to the overall dynamics of the valve [36, 37].

Selecting the state variables as, $\mathbf{x} = [x_p\ \dot{x}_p\ \ddot{x}_p]^{\mathbf{T}}$, equations (1-4) can be rewritten in the form

$$\dot{x}_1 = x_2; \tag{5}$$
$$\dot{x}_2 = x_3; \tag{6}$$
$$\dot{x}_3 = a_2\, x_2 + a_3\, x_3 + b_1\, u + d_o; \tag{7}$$

where,

$$a_2 = -\frac{b\alpha C_t}{m} - \frac{{A_p}^2}{m}\alpha\,, \qquad a_3 = -\frac{b}{m} - \alpha C_t\,,$$
$$d_o = -\frac{\alpha C_t}{m} F_d - \frac{1}{m}\dot{F}_d\,, \qquad b_1 = \frac{A_p}{m}\alpha K_q K_v\,,$$
$$\alpha = \frac{4\beta_e}{V_t}\,, \qquad K_q = C_d w\sqrt{\frac{1}{\rho}(P_s - \mathrm{sgn}(x_v)P_L)}\,.$$

Equations (5-7) describe a nonlinear state-space structure for the electro-hydraulic steering system which can be written in the general form,

$$\dot{x}_i = x_{i+1}\,,\ i = 1, \ldots, n-1;$$
$$\dot{x}_n = f(\mathbf{x}) + g(\mathbf{x}, u)u + d_o(t), \tag{8}$$

where, $f(\mathbf{x})$ is linear function of states, $g(\mathbf{x}, u)$ is nonlinear function of states and input variable, and $d_o(t)$ is the system external disturbances.

3. Grey-box System Identification.

As has been discussed in before, grey-box identification detects just the system parameters by using the system model structure obtained from basic physical principles. The next subsection illustrates the design of the input signal which is an essential stage in the identification process.

3.1. Input signal design

In order to identify all the system dynamics, the system has to be stimulated with a well-prepared input signal. Pseudo Random Multi-level Sequence (PRMS) has been used for nonlinear systems identification in numerous fields because its frequency spectrum is similar to white noise with a band limit. PRMS signal is just like the famous two-level Pseudo Random Binary Sequence (PRBS) except that its amplitude is uniformly distributed randomly within the range of interest. This is because for nonlinear systems both the frequency and amplitude contents of the input signal are important for identification process.

As with any perturbation signal with limited bandwidth the signal design parameters are chosen in such a way that the frequencies of interest can be investigated. A frequency response test was performed to determine the bandwidth for the electro-hydraulic steering system. As can be seen from Fig. 3 the bandwidth of the system is about 82.7 rad/s (13.17 Hz).

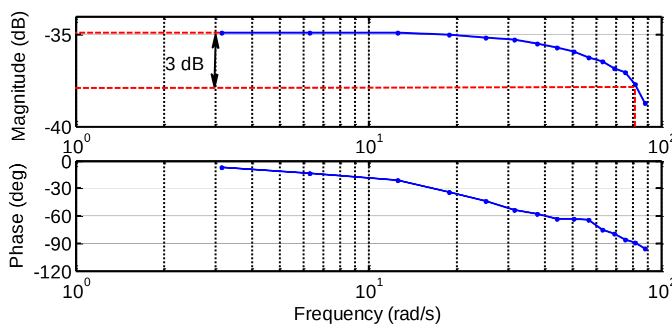

Fig. 3 Frequency response of the electro-hydraulic steering system

A PRBS generator of n-bit generates a sequence of binary pulses of random width which repeats each $N=2^n-1$ terms. The effective frequency band of PRBS is [38],

$$f_{band} = f_c\left(\frac{1}{3} - \frac{1}{N}\right), \tag{9}$$

where f_c is the PRBS clock frequency. As a general guide of choosing the value of f_c, this should be approximately 2.5 f_{max}, where f_{max} is the bandwidth maximum frequency of process under study [39], in our case it is 13.17Hz. The minimum frequency band limit of a PRBS is determined by the term 1/N in equation (9). If N is chosen too large this will lead to lengthy test time (N/f_c), since the test must remain N-terms before repeating a PRBS signal. It also causes a small reduction in the minimum limit as 1/N approaches zero. To avoid lengthy test time and meet the requirements of the minimum frequency, a 10-bits PRBS (N = 1023) signal is chosen for the current research. Finally, the designed PRBS signal is multiplied by a uniformly distributed random value within the range of the required amplitudes to get the PRMS signal. Considering the abovementioned rules, Fig. 4 and Fig. 5 show the designed PRMS and its (FFT) power spectrum. As can be noticed from Fig. 5, the intended frequency band (0.1:13.17) Hz can be achieved from the designed input signal.

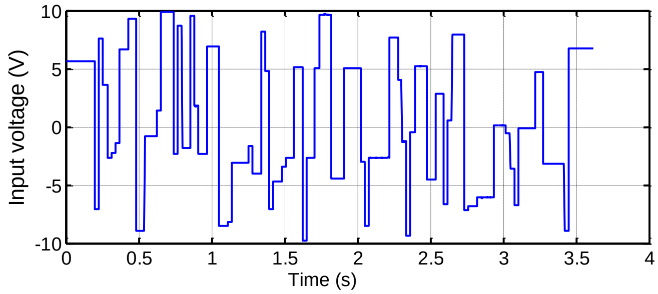

Fig. 4 Designed PRMS input signal

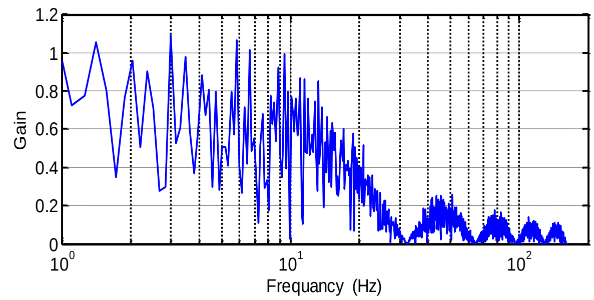

Fig. 5 Designed PRMS signal power spectrum

3.2. Experimental setup

The experiments are conducted on a front-wheel derived passenger car "FIAT Ritmo, 1979". This vehicle provides adequate space below the engine which permits the system components to be installed with little structural changes, see Fig. 6. The traditional rack and pinion mechanism is replaced by the proposed SBW system. The system mainly consists of a vane pump, a double rod hydraulic cylinder, pressure-relief valve and oil tank. The double acting cylinder is led by a solenoid-servo valve (Rexroth 4WRPEH6C4B24L-2X/G24 K0/A1M); its (0-100%) response time is ≤ 25 ms. LVDT sensor with linearity of about ± 0.1% is used to measure the position feedback signal of the cylinder.

The designed PRMS signal is provided by SIMULINK/MATLAB of MathWorks company and sent, using data acquisition card (NI-6036-PCI), to the solenoid-servo valve. PC is used for real-time processing of the signals and control algorithm. The PRMS signal and the cylinder position feedback signal are recorded in the host PC to be used in system identification. For experimental work, a sample time of 0.001 s was used, which is acceptable for most servo-hydraulic systems [40].

3.3. System identification and model verification

Fig. 7 shows the velocity of the hydraulic cylinder when the system is stimulated by the designed PRMS signal. The response is recorded along with the input signal. This input-output data, as well as the model structure provided by equations (5-7) are used to estimate the system's unknown parameters using system identification. The Prediction Error Minimization (PEM) estimation technique was used to get the model parameters. PEM is an iteration-based method in which the parameters are selected best to decrease the error between the real-time signal and the expected one. The method is applied using system identification toolbox by MATLAB. It is found that, the system dynamics is best described by the following model:

$$\begin{aligned} \dot{x}_1 &= x_2; \\ \dot{x}_2 &= x_3; \\ \dot{x}_3 &= -5779\,x_2 - 112\,x_3 + 78.0617\,u. \end{aligned} \tag{10}$$

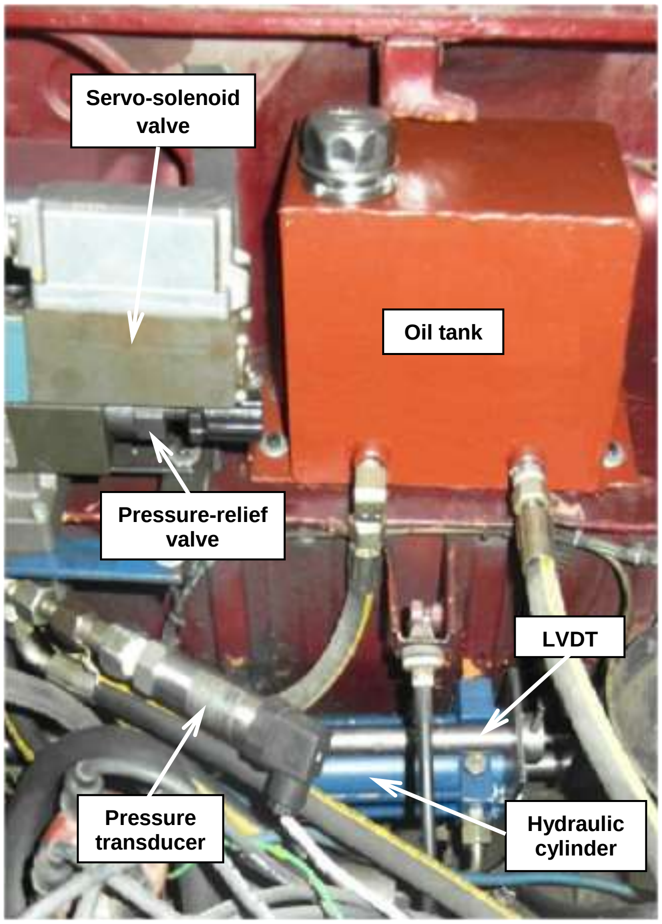

Fig. 6. Electro-hydraulic steering system inside the test vehicle

Fig. 8 shows the cylinder velocity, calculated from the identified model, and that of the real system. The results show that both signals are comparable, as the model catches the basic dynamic features. Frequency response analysis is another method for validating mathematical models since it shows the process dynamics in a clear manner. Fig. 9 shows a comparison between the frequency responses of the model identified and that of the real system. As can be noticed, there are little discrepancies between the two responses, however the main trends are the same.

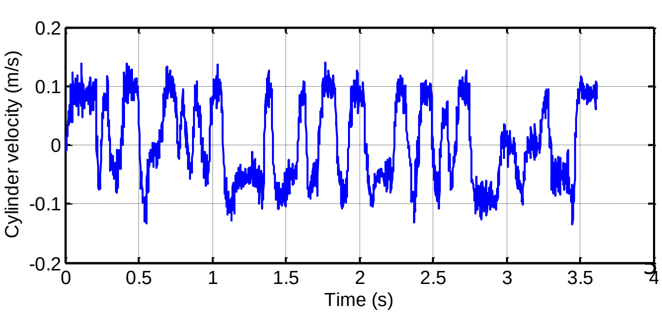

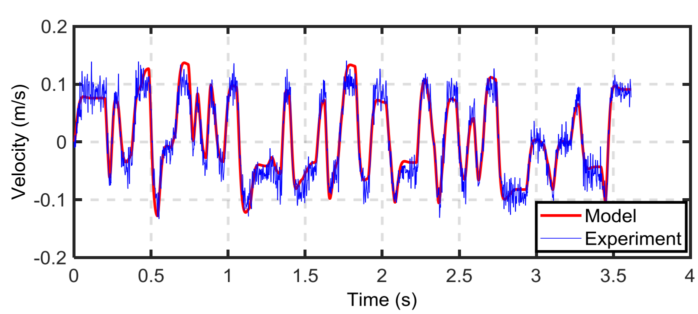

Fig. 7 Hydraulic cylinder velocity as a response of the input PRMS signal

Fig. 8 Comparison between the outputs of the identified model and the real system

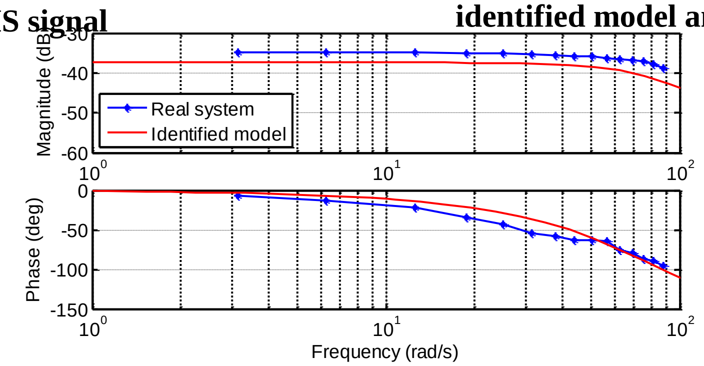

Fig. 9 Frequency response of the physical system and the identified model

4. Sliding Mode Control

Insensitivity to parameters uncertainty and external disturbances have made SMC good candidate controller for the position tracking of the electro-hydraulic steering system. The designing of SMC consists of two steps. The first step is to design sliding surface, s(x), through which the desired dynamic performance of the controlled system is prescribed. The second step is constructing a control law necessary to drive the system states to the sliding surface and satisfying the generalized Lyapunov stability theory [41].

Considering the system mathematical model driven in section (2), equation (8) can be written in terms of the identified model (10) as,

$$\dot{x}_3 = f(\mathbf{x}) + \Delta f(\mathbf{x}) + g_1 u + \Delta g(\mathbf{x}, u) + d_o(t), \qquad (11)$$

where, $f(\mathbf{x}) = -5779\, x_2 - 112\, x_3$, $g_1 = 78.0617$, $\Delta f(\mathbf{x})$ and $\Delta g(\mathbf{x}, u)$ are uncertainties between derived and identified models. We rewrite (11) as,

$$\dot{x}_3 = f(\mathbf{x}) + g_1 u + q(\mathbf{x}, u, t), \qquad (12)$$

where, $q(\mathbf{x}, u, t) = \Delta f(\mathbf{x}) + \Delta g(\mathbf{x}, u) + d_o(t)$ and $|q(\mathbf{x}, u, t)| \leq D$, D is a positive constant value. Since the plant is of the third order, sliding surface can be chosen as,

$$s = c_2 e + c_1 \dot{e} + \ddot{e} \qquad (13)$$

where, e is tracking error,

$$e = x_d - x_p, \tag{14}$$

and x_d is the desired position trajectory. The parameters c_1 and c_2 are chosen to satisfy Hurwitz condition. From (13) we get,

$$\dot{s} = c_2\dot{e} + c_1\ddot{e} + \dddot{e} ,$$

or,

$$\dot{s} = c_2\dot{e} + c_1\ddot{e} + \dddot{x}_d - \dddot{x}_p. \tag{15}$$

Substituting for $\dddot{x}_p$ from (12) gives,

$$\dot{s} = c_2\dot{e} + c_1\ddot{e} + \dddot{x}_d - f(\mathbf{x}) - g_1u - q(\mathbf{x}, u, t). \tag{16}$$

Using reaching law of the form,

$$\dot{s} = -\eta\ \mathrm{sat}(s),\ \ \eta > 0, \tag{17}$$

and equating (16) and (17), gives,

$$c_2\dot{e} + c_1\ddot{e} + \dddot{x}_d - f(\mathbf{x}) - g_1u - q(\mathbf{x}, u, t) = -\eta\ \mathrm{sat}(s). \tag{18}$$

A saturated function sat(s) is used here in order to minimize the chattering phenomenon in the control signal [41], where,

$$\mathrm{sat}(s) = \begin{cases} 1, & s > \Delta \\ s/\Delta, & |s| \le \Delta \\ -1, & s < -\Delta \end{cases}, \tag{19}$$

and Δ is a chosen boundary layer.

Neglecting $q(\mathbf{x}, u, t)$ and solving for the control signal u we get,

$$u(t) = \frac{1}{g_1}[c_2\dot{e} + c_1\ddot{e} + \dddot{x}_d - f(\mathbf{x}) + \eta\ \mathrm{sat}(s)]. \tag{20}$$

Define a Lyapunov function as,

$$L = \frac{1}{2}s^2. \tag{21}$$

Therefore, according to Lyapunov stability criterion,

$$\dot{L} = s\dot{s} \le 0, \tag{22}$$

it follows that,

$$\dot{L} = s[c_2\dot{e} + c_1\ddot{e} + \dddot{x}_d - f(\mathbf{x}) - g_1u - q(\mathbf{x}, u, t)] \le 0. \tag{23}$$

Substituting the control signal (20) into (23) yields,

$$s(-q(\mathbf{x}, u, t) - \eta\ \mathrm{sat}(s)) \le 0. \tag{24}$$

Therefore, to satisfy the stability condition,

$$-s\, q(\mathbf{x}, u, t) - \eta|s| \le 0,$$

or

$$\eta \ge |q(\mathbf{x}, u, t)|. \tag{25}$$

5. Experimental Evaluation

The experimental setup used for the validation of the proposed controller is shown in Fig 10. he setup, as discussed in section 3.2, which is used for identification process except the host PC which is now utilized in real time mode to implement the control algorithm. A test is conducted on the system to assess the time delay associated with signal processing in various electrical devices. Therefore, input-output data was monitored using oscilloscope; a time delay of 0.002 s was recorded.

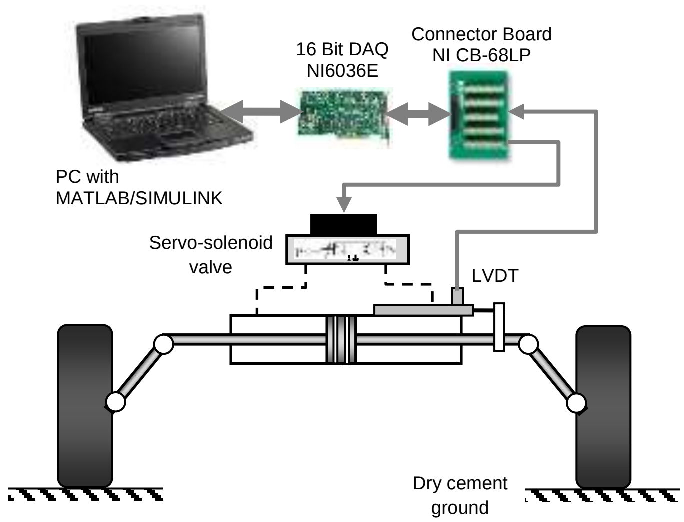

Fig. 10 Schematic diagram of the experimental setup

Before applying the control algorithm, SIMULINK is used to help choosing controller parameters explained in equations (19), (20) and (25). The parameters η and Δ were selected to keep chattering level as low as possible and the control signal u within the saturation limits (±10 V). The parameters c_1 and c_2 are chosen to satisfy Hurwitz criterion and to minimize (as possible) system overshoot. Table (1) shows the designed parameters of the SMC which are utilized in the current research.

Table 1 SMC parameters

Parameter	Value
c_1	80
c_2	1600

η	200
Δ	0.5

To evaluate the performance of position tracking algorithm, a reference input has been designed to test the system under high steering rate conditions. Among many automobile drivers the greatest steering-wheel rate ranges between 600 and 800 degrees per second [42]. Therefore, a rate of 720 degree/s was chosen as a reasonable typical figure within this range. This is equivalent to 7.5 cm/s piston velocity according to the test car's steering ratio. Hence, a reversal ramp signal with the above-mentioned rate was created and applied to the system. The experiments were conducted on two groups. The first one was with no disturbance force and achieved by lifting the vehicle off the ground. The second one took into account the external disturbances and was achieved by resting the vehicle on a cement ground.

5.1. System performance – no-load condition

Fig. 11 shows the system response under no force disturbances when it is given the reversal ramp signal. As can be observed, the steering mechanism tracks the reference signal accurately. A close-up of the reference signal's rapid shift zone (Fig. 12) reveals an overshoot of 4.16% and a settling time of about 0.1 sec.

It is also important to test the tracking performance of the steering controller at different steering frequencies. Two additional reference signals were created for this reason. The first is a sinusoidal input of 96 degrees amplitude and 1 Hz frequency. This equals to a 1 cm amplitude movement of the hydraulic cylinder. The amplitude was reduced to 48 degrees and the frequency was raised to 2 Hz in the second test. This simulates a driving situation in which the vehicle is heavily manipulated (for instance, avoiding an unexpected barrier on a highway). Figures 13–16 depict the controller's behaviour without external load disturbances. As can be noticed, the steering system presents good tracking to the reference signal. As the frequency rises, so does the tracking inaccuracy. At frequency of 2 Hz, the greatest tracking error was 0.025 cm amplitude (2 degrees of steering wheel) and the phase shift was 0.012 s. As can be observed in Fig. 14 and Fig. 16, all of the control inputs were found within the prescribed limits (10 V). However, a modarate-level chattering phenomenon is noticed in the figures. By choosing a wider boundary layer Δ, this chattering is reduced greatly, yet, the tracking error is increased. The result shown in Fig. 14 and Fig. 16 is a compromise.

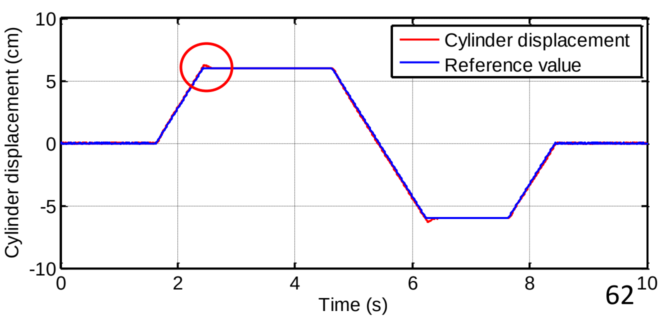

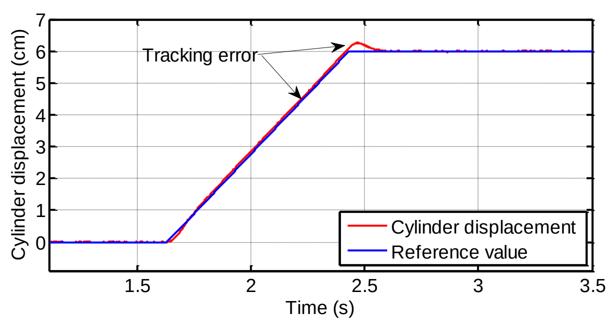

Fig. 11 Tracking performance for reversal ramp signal without external force

Fig. 12 Close-up on sudden change zone in Fig. 11

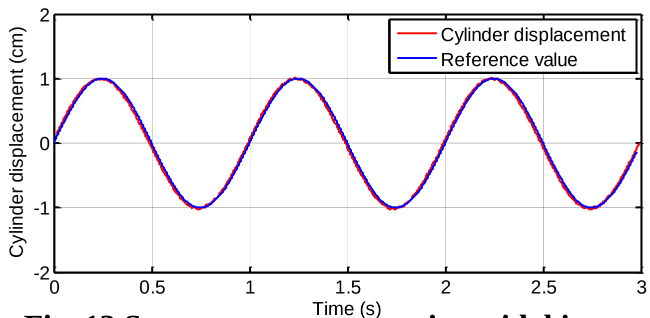

Fig. 13 System response to a sinusoidal input of 1 Hz frequency and 1 cm amplitude without external load disturbances

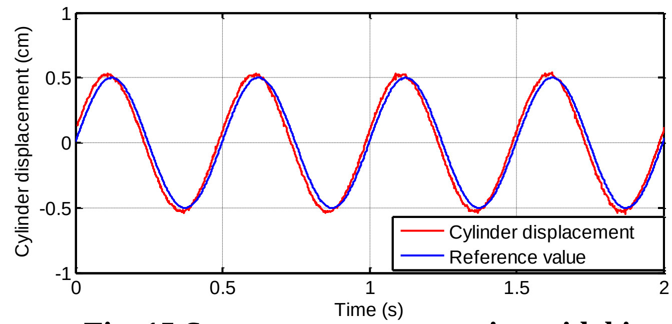

Fig. 15 System response to a sinusoidal input of 2 Hz frequency and 0.5 cm amplitude without external load disturbances

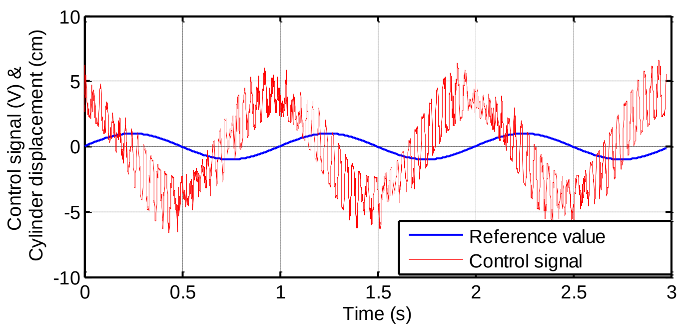

Fig. 14 Control signal for a sinusoidal input of 1 Hz frequency and 1 cm amplitude without external load disturbances

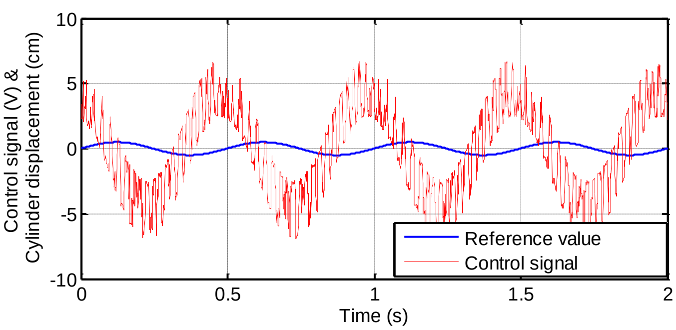

Fig. 16 Control signal for a sinusoidal input of 2 Hz frequency and 0.5 cm amplitude without external load disturbances

5.2. System performance in the presence of external disturbance

The second test group was done after placing the car on a concrete ground. To assess the tracking ability under this condition the system is tested by the same three mentioned-above reference inputs. Fig. 17 through Fig. 22 illustrate the system performance. As can be seen, despite the fact that force disturbance is implemented, the controller still maintains a high level of precision. The overshoot percentage, as seen in Fig. 18, decreased to 3% compared to the no disturbance case (4.16%). This is caused by the dapming effect introduced to the system by the tire-ground interaction. The settling time remains unchanged (≈ 0.1 s).

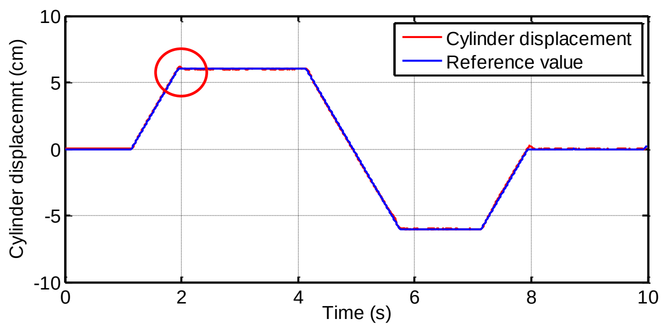

Fig. 17 Tracking behavior for a ramp signal with external load disturbances

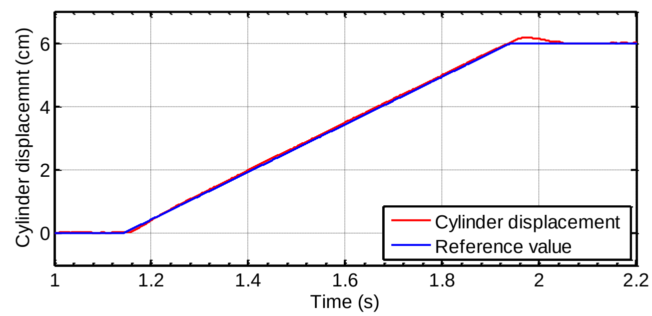

Fig. 18 Close-up on sudden change zone in Fig. 17

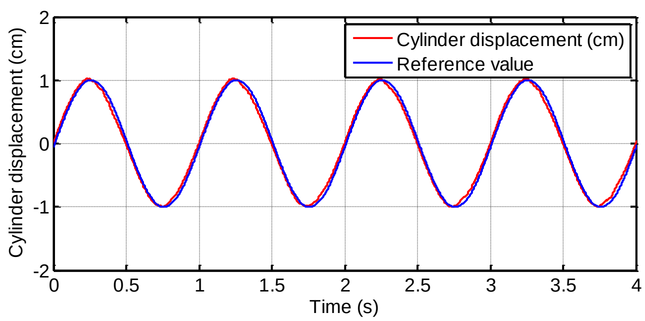

Fig. 19 System response to a sinusoidal input of 1 Hz frequency and 1 cm amplitude with external load disturbances

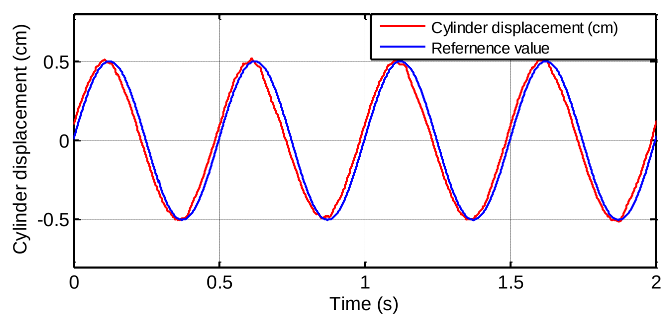

Fig. 21 System response to a sinusoidal input of 2 Hz frequency and 0.5 cm amplitude with external load disturbances

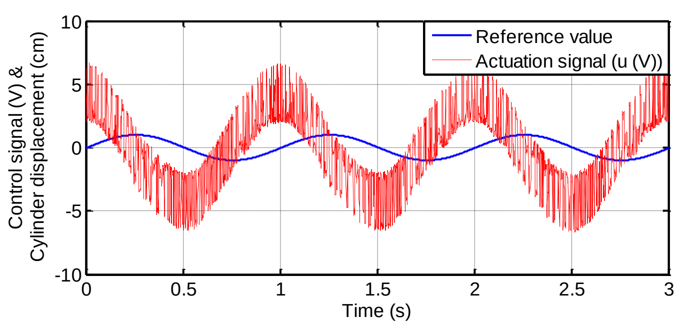

Fig. 20 Control signal for a sinusoidal input of 1 Hz frequency and 1 cm amplitude with external load disturbances

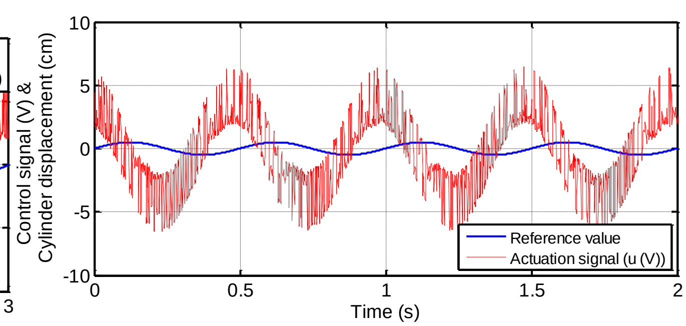

Fig. 22 Control signal for a sinusoidal input of 2 Hz frequency and 0.5 cm amplitude with external load disturbances

Other tests involving steering with varying frequencies are depicted in Figs. 19–22. The maximum tracking error is recorded in the case of sinsuidal input of 2 Hz frequency. The error is 0.015 cm (≈ 1.5 degree of steering wheel rotation) and a phase shift of 0.015 s (instead of 0.012 s in case of no distubances). Figures 20 and 22 show that the control inputs are all within the 10 V limit. However, the chattering phenomenon has increased in comparison to the no-disturbance case. It is believed that, this chattering is due to fast unmodeled dynamics in the identified model. These dynamics with small time constant changes the error trajectory. Therefore, in order to maintain minimum tracking error and smooth control input the width of the boundary layer should also be changed.

6. Conclusion

In this research, modeling and variable structure control of the electro-hydraulic SBW system was investigated. Grey-box system identification techniques were used to identify the model's parameters. Simulations were used to construct and tune a fixed boundary-layer SMC. Finally, tests in a real-time setting were used to validate the suggested controller. The experiments were conducted with the existence of strong external disturbances and at high steering rates and frequencies. The proposed controller showed stability and capability to track the reference signals with high accuracy even in the presence of high external disturbances. At high steering rate (720 degree/s) the maximum overshoot is found to be 3% with a setling time of 0.1 s. However, a modarate-level chattering phenomenon was noticed. In order to reduce the chattering phenomenon and keep the accuracy of the tracking performance, a SMC, in which the boundary layer width varies adaptively, is recommended.

References

[1] Nguyen B-H, Ryun J-H. Direct current measurement-based steer by wire systems for realistic driving feeling. IEEE International symposium on industrial electronics; 2009. p. 1023-28.
[2] Jang S, Park T, Han C. A control of vehicle using steer-by-wire system with hardware-in-the-loop-simulation system. Proceedings of IEEE/ASME international conference on advanced intelligent mechatronics; 2003. p. 389-94.
[3] Daher N, Ivantysynova M. A Steer-by-wire System that Enables Remote and Autonomous Operation. SAE 2014 Commercial vehicle engineering congress, Rosemont, IL, USA. SAE Technical Paper No. 2014-01-2404.
[4] Karpenko M, Sepehri N. Hardware-in-the-loop simulator for research on fault tolerant control of electro-hydraulic actuators in a flight control application. Mechatronics 2009;19(7):1067–77.
[5] Wu M, Shih M. Simulated and experimental study of hydraulic anti-lock braking system using sliding-mode PWM control. Mechatronics 2003;13(4):331–51.

[6] Sam Y, Osman J, Ghani M. A class of proportional-integral sliding mode control with application to active suspension system. Systems and Control Letters 2004;51(3-4):217–23.
[7] Chiang M, Huang C. Experimental implementation of complex path tracking control for large robotic hydraulic excavators. International Journal of Advanced Manufacturing Technology 2004;23(1-2):126–32.
[8] Renn J, Tsai C. Development of an unconventional electro-hydraulic proportional valve with fuzzy-logic controller for hydraulic presses. International Journal of Advanced Manufacturing Technology 2005;26(1-2):10–16.
[9] Chiang M., Yeh Y, Yang F, Chen Y. Integrated control of clamping force and energy-saving in hydraulic injection moulding machines using decoupling fuzzy sliding mode control. International Journal of Advanced Manufacturing Technology 2005;27(1-2):53–62.
[10] Jha S, Jain V. Design and development of the magnetorheological abrasive flow finishing (MRAFF) process. International Journal of Machine Tools and Manufacture 2004;44(10):1019–29.
[11] Merritt HE. Hydraulic control systems. New York: John Wiley & Sons; 1967.
[12] Kroll A. Grey-box models and their application to a steel mill. In CIMCA; 1999. p. 340–45.
[13] Plummer AR, Vaughan AD. Decoupling pole-placement control, with application to a multi-channel electro-hydraulic servo system. Control Eng Pract 1997;5(3):313–23.
[14] Lim T. Pole Placement Control of an Electro-hydraulic Servo Motor. In Proc. of 2nd Int. Conf. Power Electronic Drive System; 1997, Part 1, Vol. 1, p. 350-56.
[15] Ishak N, Tajjudin M, Ismail H, Rahiman M, Sam Y, Adnan R. PID Studies on Position Tracking Control of an Electro-Hydraulic Actuator. International Journal of Control Science and Engineering; 2012, Vol. 2 No. 5, p. 120-26.
[16] Bobrow JE, Lum K. Adaptive, high bandwidth control of a hydraulic actuator. ASME J Dyn Syst Meas, Control 1996;118(4):714– 20.
[17] Ghazali R, Sam Y, Rahmat M, Zulfatman, Hashim A. Simulation and experimental studies on perfect tracking optimal control of an electro-hydraulic actuator system. Journal of Control Science and Engineering 2012. http://dx.doi.org/10.1155/2012/670635.
[18] Seo J, Venugopal R, Kenne J-P. Feedback linearization based control of a rotational hydraulic drive. Control Eng Pract 2007;15(12):1495–07.
[19] Mintsa H, Venugopal R, Kene J, Belleau C. Feedback linearization-based position control of an electro-hydraulic servo system with supply pressure uncertainty. IEEE Trans. Control Syst. Technol. 2012;20(4):1092–99.
[20] Vossoughi G, Donath M. Dynamic feedback linearization for electro-hydraulically actuated control systems. ASME J Dyn Syst Meas Control 1995;117(4):468–77.

[21] Liccardo F, Strano S, Terzo M. Optimal control using state-dependent riccati equation (SDRE) for a hydraulic actuator. Proceedings of The World Congress on Engineering; 2013. p. 2003-07.
[22] Çimen T. Survey of state-dependent riccati equation in nonlinear optimal feedback control synthesis. AIAA Journal of Guidance, Control, and Dynamics 2012;35(4):1025–47.
[23] Kim HM, Park SH, Song JH, Kim JS. Robust position control of electro-hydraulic actuator systems using the adaptive back-stepping control scheme. J Syst Control Eng 2010;224:737–46.
[24] Ahn KK, Doan NCN, Maolin J. Adaptive backstepping control of an electrohydraulic actuator. IEEE Trans Mechatronics 2014;19(3):987–95.
[25] Tri NM, Nam DNC, Park HG, Ahn KK. Trajectory control of an electro hydraulic actuator using an iterative backstepping control scheme. doi:10.1016/j.mechatronics.2014.10.002
[26] Bonchis A, Corke PI, Rye DC, Ha QP. Variable structure methods in hydraulic servo systems control. Automatica 2001;37(4):589–95.
[27] Wonhee K, Donghoon S, Daehee W, Chung CC. Disturbance-observer-based position tracking controller in the presence of biased sinusoidal disturbance for electro-hydraulic actuators. IEEE Trans Control Syst Technol 2013;21(6):2290–8.
[28] Guo K et al. Position tracking control of electro-hydraulic single-rod actuator based on an extended disturbance observer. Mechatronics 2015;27, (April 2105):47-56.
[29] Yang L, Yang S, Burton R. Modeling and robust discrete-time sliding-mode control design for a fluid power electrohydraulic actuator (EHA) system. IEEE/ASME Trans Mech 2013;18(1):1–10.
[30] Cheng G, Shuangxia P. Adaptive sliding mode control of electro-hydraulic system with nonlinear unknown parameters. Control Eng Practice 2008;16(11):1275–84.
[31] Tang R, Zhang Q. Dynamic sliding mode control scheme for electro-hydraulic position servo system. Proc Eng 2011;24:28–32.
[32] Chaudhuri S, Mookherjee S, Sanyal D. Adaptive force tracking in electrohydraulic system with first order sliding mode control. Proceedings of IEEE first international conference on control, measurement and instrumentation (CMI); 2016. P. 300-304.
[33] Shaer B, Kenne J-P, Kaddissi C and Fallaha C. A chattering-free fuzzy hybrid sliding mode control of an electrohydraulic active suspension. Transactions of the Institute of Measurement and Control, 2016, DOI: 10.1177/0142331216652468.
[34] Das Mahapatra S, Saha R, Sanyal D, Sengupta A, Bhattacharyya U and Sanyal S. Designing low-chattering sliding mode controller for an electrohydraulic system. Proceedings of IEEE first international conference on control, measurement and instrumentation (CMI); 2016. P. 316-320.
[35] Tian Q, Wei J, Fang J and Guo K. Adaptive fuzzy integral sliding mode velocity control for the cutting system of a trench cutter. Frontiers of Information Technology & Electronic Engineering; 2016; 17(1): 55-66

[36] Chen H.-M., et al., Sliding mode control with varying boundary layers for an electro-hydraulic position servo system. The International Journal of Advanced Manufacturing Technology 2005; 26(1-2): 117-123.
[37] Rahmat M., et al., Modeling and controller design of an industrial hydraulic actuator system in the presence of friction and internal leakage. International Journal of Physical Sciences 2011; 6(4): 3502-3517.
[38] Davies W. System identification for self-adaptive control. London: Wiley-Interscience; 1970.
[39] Pintelon R, Schoukens J. System identification: a frequency domain approach. New York: IEEE Press; 2001.
[40] Reuter H. Zur Identifikation nichtlinearer Systemmodelle mit wenig A-priori-Informationen. Fortschritt-Berichte. Reihe 8 Nr. 471, Düsseldorf: VDI-Verlag 1995.
[41] Liu J and Wang X. Advanced sliding mode control for mechanical systems. Springer-Verlag Berlin Heidelberg; 2012.
[42] Kebschull B, Ishii K, Ernst M. Rollover resistance test procedure involving maximum roll momentum. Proceedings of the 18th International Technical Conference on the Enhanced Safety of Vehicles (ESV); 2003.